

Conference Paper

Study on the Flow and Heat Transfer Characteristics in the Tube Side of Spiral-Wound Heat Exchanger

S. L. Li¹, W. H. Cai¹, H. C. Zhang¹, and Y. Q. Jiang^{2,3}¹School of Energy Science and Engineering, Harbin Institute of Technology, Harbin, China²School of Architecture, Harbin Institute of Technology, Harbin, China³Heilongjiang Provincial Key Laboratory of Building Energy Efficiency and Utilization, Harbin, China

Abstract

In this article, the characteristics of hydrocarbons condensation flow and heat transfer in tube-side of spiral wound heat exchanger under static and sloshing conditions were numerically investigated based on the verified model. It is shown that at static conditions, as the vapor quality increases, the heat transfer coefficient first increases and then decreases, whereas the frictional pressure drop always increases. The pure hydrocarbon shows better flow and heat transfer performances than hydrocarbon mixture. Moreover, sloshing motions could bring about both drag reduction and heat transfer enhancement. These results are helpful to understand condensation flow in a spiral pipe.

Corresponding Author:

W. H. Cai

caiwh@hit.edu.cn

Received: 14 September 2018

Accepted: 1 October 2018

Published: 14 October 2018

Publishing services provided by
Knowledge E

© S. L. Li et al. This article is distributed under the terms of the [Creative Commons Attribution License](#), which permits unrestricted use and redistribution provided that the original author and source are credited.

Selection and Peer-review under the responsibility of the ASRTU Conference Committee.

Keywords: hydrocarbons, condensation, spiral pipe, sloshing motion

1. Introduction

Spiral wound heat exchanger (SWHE) (Figure 1) has been widely used as a main cryogenic exchanger in large-scale liquid natural gas (LNG) plants owing to its different advantages, such as multi-stream capability, high compactness, efficient heat transfer, sufficient flexibility, and better robustness among others [1, 2]. It also has a great potential in floating liquefied natural gas (FLNG) field. Meanwhile, hydrocarbons are usually used as a working medium in LNG field. Therefore, a better understanding of condensation flow and heat transfer for hydrocarbons in a spiral pipe under static and sloshing conditions can be contributed to the design and optimization of SWHE used in FLNG field.

Some investigations have been carried out on condensation flow and heat transfer characteristics in helically coiled tubes. Wongwises et al. [3] experimentally studied

OPEN ACCESS

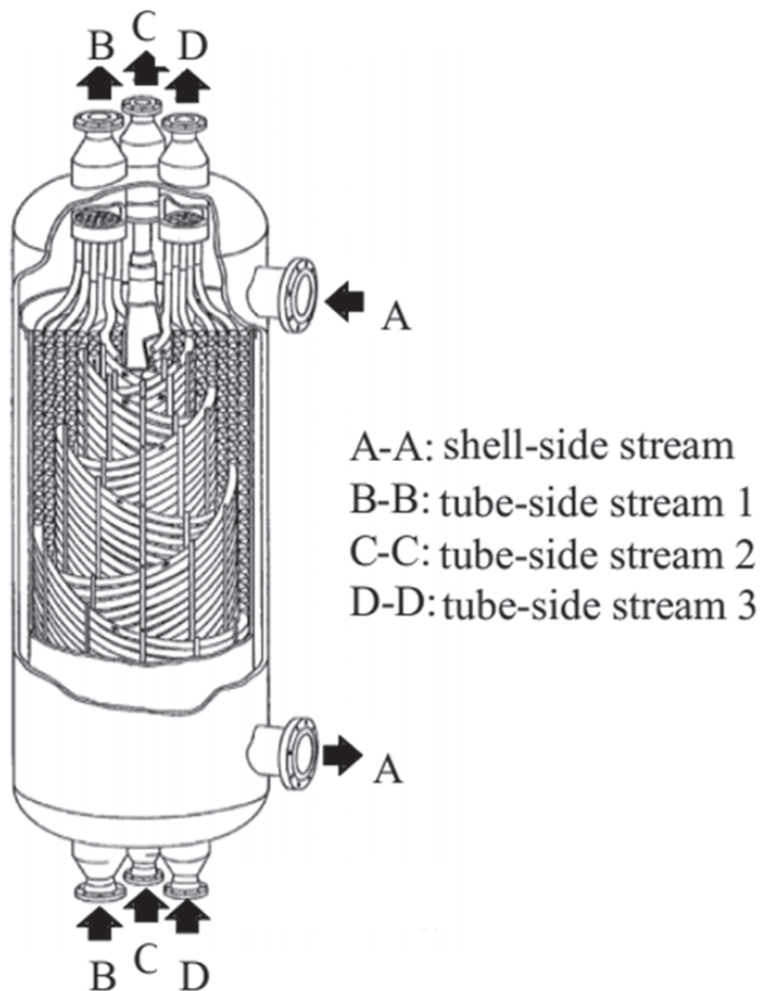


Figure 1: A schematic of a multi-stream SWHE.

condensation heat transfer and pressure drop of R134a in a helically tube and found that they were both larger than those in a straight tube, which was also found in Gupta et al.'s study [4]. Mozafari et al. [5] investigated the effects of different orientations of helical pipe on condensation heat transfer and pressure drop of R600a; the results showed that it had a significant effect on them. Salimpour et al. [6] suggested that condensation heat transfer coefficients of R404A in helically coiled tubes increased with the decreasing coil diameter and coil pitch. Li et al. [7, 8] established a numerical model to study the condensation flow and heat transfer characteristics of propane and ethane/propane mixture in a spiral pipe and compared their simulation results with experimental ones. It could be clearly seen that the deviations between simulation results and experimental ones [9] were within 15%, which proved the rationality of the model.

At the same time, there have been some studies in literature on flow and heat transfer under sloshing conditions. Tan et al. [10] investigated single-phase natural

circulation flow and heat transfer under rolling conditions. It was shown that the rolling motion could cause heat transfer enhancement, while the effect increased with the increase of rolling amplitude and frequency. Yu et al. [11] found that the fluctuations of frictional pressure drop and flow rate were synchronous. Jin et al. [12] investigated the flow resistance of air–water flow under rolling conditions. It stated the fluctuation amplitude of two-phase frictional pressure drop increased with the rise in vapor quality and rolling amplitude and the drop in Reynolds number. Chen et al. [13, 14] discussed the effect of rolling motion on frictional pressure drop and heat transfer for boiling flow. It demonstrated that the fluctuation amplitudes both increased as the rolling amplitude, rolling period, and heat flux increased and the system pressure decreased.

The aforementioned surveys indicate that few studies have been devoted to the hydrocarbons condensation in a spiral pipe under sloshing conditions. Therefore, in this article, firstly, a numerical model was proposed and verified by experimental data. Then, the characteristics of hydrocarbons condensation flow and heat transfer in SWHE tube side under static and sloshing conditions were both discussed and some important conclusions were drawn.

2. Methods

A computational model (Figure 2) was established to simulate hydrocarbons condensation upward flow in a spiral pipe. It contains 0.6 m developing section, 0.2 m test section, and 0.2 m regulator section. The hydraulic diameter, curvature diameter, and helix angle are 10 mm, 2 m, and 10° , respectively. The mass flow, static pressure, and constant heat flux were adopted at inlet, outlet, and wall, respectively. The working fluids are methane (C1) and methane/ethane/propane (C1C2C3). All physical properties were gained by REFPROP [15].

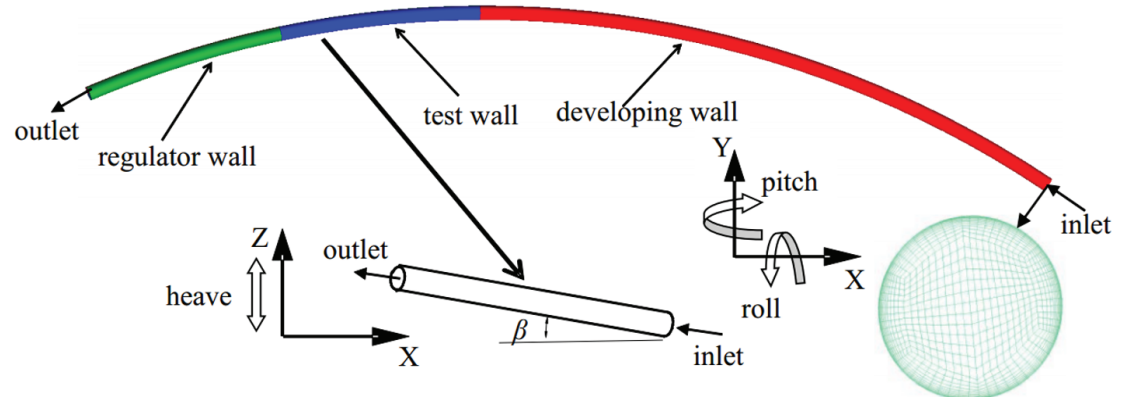


Figure 2: Computational model and mesh of a spiral pipe.

2.1. Governing equations

In this article, the inhomogeneous two-fluid model together with standard $k-\epsilon$ turbulence model and thermal phase change model was adopted. The governing equations are shown as:

$$\frac{\partial}{\partial t} (\alpha_l \rho_l) + \nabla \cdot (\alpha_l \rho_l \vec{u}_l) = \Gamma_{lv}, \quad \frac{\partial}{\partial t} (\alpha_v \rho_v) + \nabla \cdot (\alpha_v \rho_v \vec{u}_v) = \Gamma_{vl} \quad (1)$$

$$\frac{\partial}{\partial t} (\alpha_l \rho_l \vec{u}_l) + \nabla \cdot (\alpha_l \rho_l \vec{u}_l \vec{u}_l) = \alpha_l (\rho_l - \rho_{ref}) \vec{g} + \nabla \cdot \left\{ \alpha_l (\mu_l + \mu_{tl}) \left[\nabla \vec{u}_l + (\nabla \vec{u}_l)^T \right] \right\} - \alpha_l \nabla p + \vec{F}_{lv} \quad (2)$$

$$\frac{\partial}{\partial t} (\alpha_v \rho_v \vec{u}_v) + \nabla \cdot (\alpha_v \rho_v \vec{u}_v \vec{u}_v) = \alpha_v (\rho_v - \rho_{ref}) \vec{g} + \nabla \cdot \left\{ \alpha_v (\mu_v + \mu_{tv}) \left[\nabla \vec{u}_v + (\nabla \vec{u}_v)^T \right] \right\} - \alpha_v \nabla p + \vec{F}_{vl} \quad (3)$$

$$\frac{\partial}{\partial t} (\alpha_v \rho_v \gamma_v) + \nabla \cdot (\alpha_v \rho_v \vec{u}_v \gamma_v) = \nabla \cdot (\alpha_v \lambda_v \nabla T_v) + q_v + \Gamma_{vl} \gamma_{vS} \quad (4)$$

$$\frac{\partial}{\partial t} (\alpha_l \rho_l \gamma_l) + \nabla \cdot (\alpha_l \rho_l \vec{u}_l \gamma_l) = \nabla \cdot (\alpha_l \lambda_l \nabla T_l) + q_l + \Gamma_{lv} \gamma_{lS}, \quad (5)$$

where

$$\Gamma_{lv} = (q_v + q_l) / (\gamma_{vS} - \gamma_{lS}), \quad q_l = h_l A_{lv} (T_S - T_l), \quad q_v = h_v A_{lv} (T_S - T_v), \quad (6)$$

where A_{lv} is the interfacial area density between liquid phase and vapor phase

$$A_{lv} = \alpha_v \alpha_l / d_{lv}, \quad (7)$$

where d_{lv} represents the mean interfacial lengths scale, as shown in [7]:

$$d_{lv} = \sqrt{(1 - \zeta) \overline{Nu_{lv} \lambda_{tp} \alpha_v \alpha_l} L d \gamma_{lv} / [(8 |q| C p_l L \xi + 2m(1 - x) C p_l d \gamma_{lv}) \zeta]} \quad (8)$$

2.2. Sloshing model

In this article, the function of the sloshing motion is as follows:

$$\begin{aligned} z(t) &= z_{\max} \sin(2\pi t/t_c), v_z(t) = z_{\max} (2\pi/t_c) \cos(2\pi t/t_c), a_z(t) \\ &= -z_{\max} (2\pi/t_c)^2 \sin(2\pi t/t_c) \\ \theta(t) &= \theta_{\max} \sin(2\pi t/t_c), \omega(t) = \theta_{\max} (2\pi/t_c) \cos(2\pi t/t_c), \beta(t) \\ &= -\theta_{\max} (2\pi/t_c)^2 \sin(2\pi t/t_c) \end{aligned} \quad (9)$$

where z_{\max} (θ_{\max}) denotes sloshing amplitudes, t_c is a sloshing cycle.

The sloshing simulations were achieved by adding an additional force in Eqs. (2, 3), as:

$$\vec{F}_{sloshing,i} = -\alpha_i \rho_i \vec{a}_z(t), \text{ heave; } \vec{F}_{sloshing,i} = -\alpha_i \rho_i \vec{\beta}(t) \times \vec{r}, \text{ roll or pitch} \quad (10)$$

2.3. Model verification

In order to verify the rationality of the model, the comparison between simulated frictional pressure drop and heat transfer coefficient and experimental ones for methane/propane mixture are shown in Figure 3. It can be found that they both coincide with experimental ones at static and sloshing conditions, which indicates the applicability of the used model.

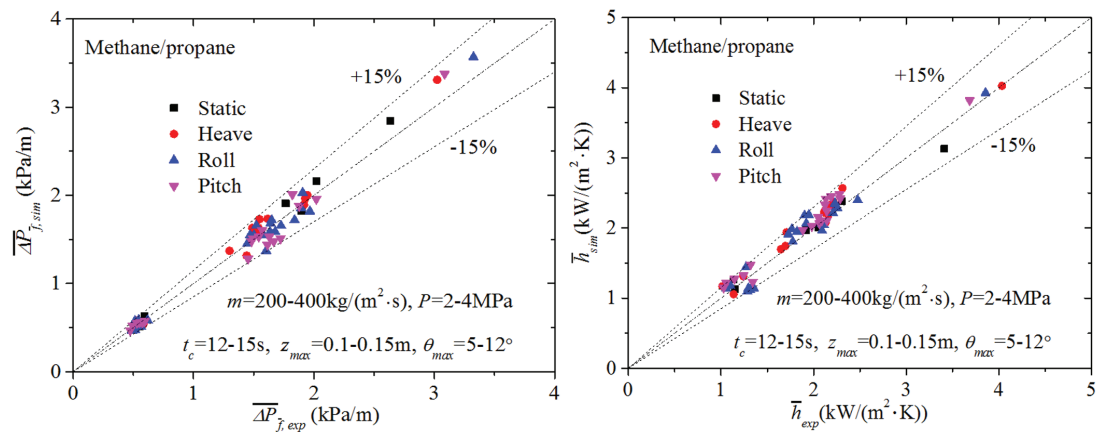


Figure 3: Comparison between simulation results and experimental ones at static and sloshing conditions under different sloshing and operating parameters: (a) time-averaged frictional pressure drop; (b) time-averaged heat transfer coefficient.

3. Results

3.1. Condensation pressure drop and heat transfer at static conditions

Figure 4(a) displays the variation of the frictional pressure drop with vapor quality for C1 and C1C2C3 at static conditions. It can be found that for both pure and mixture hydrocarbons, the frictional pressure drop always increases with the increasing vapor quality since as the vapor quality increases, the vapor-liquid velocity ratio increases and shear effect enhances. Meanwhile, at a given vapor quality, the frictional pressure drop of C1C2C3 is always larger than that of C1 due to the larger liquid-vapor density ratio and liquid viscosity for C1C2C3.

Figure 4(b) gives out the heat transfer coefficient varying with vapor quality for C1 and C1C2C3 at static conditions. The results suggest that the heat transfer coefficients of C1 and C1C2C3 both first increase and then decrease as the vapor quality increases, while the maximum value appears, when the vapor quality is 0.75. This is because the larger vapor quality will cause larger void fraction and thinner liquid film, leading to a

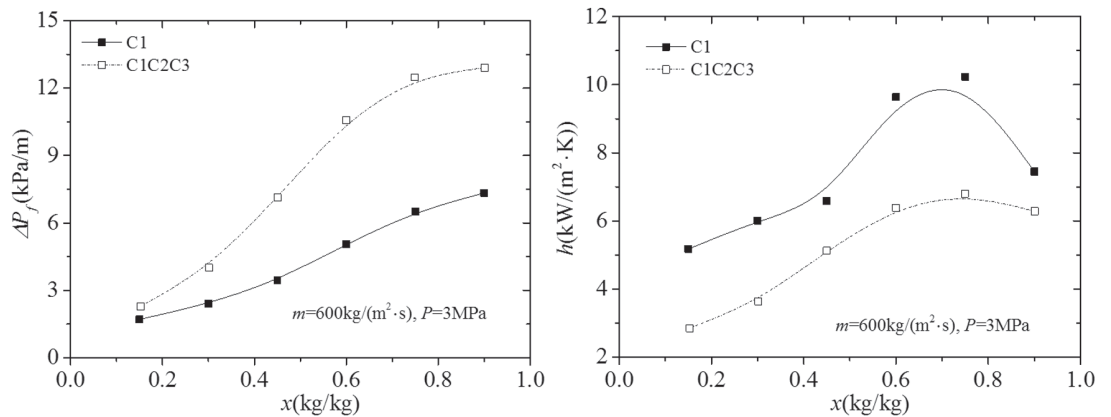


Figure 4: (a) Frictional pressure drop and (b) heat transfer coefficient versus vapor quality at static condition for C1 and C1C2C3.

smaller thermal resistance, but when the vapor quality is large enough, the appearance of partial drying on the wall will cause heat transfer deterioration. Besides, at a given case, the heat transfer of C1C2C3 is worse than that of C1 because of heat and mass transfer thermal resistance for C1C2C3.

3.2. Condensation pressure drop and heat transfer at sloshing conditions

The transient relative frictional pressure drop and heat transfer coefficient under different sloshing conditions for C1 are plotted versus time in Figures 5(a) and (b), respectively. The results explain that the relative frictional pressure drop and heat transfer coefficient both change periodically with time under different sloshing conditions. Concurrently, compared to those under static conditions, the frictional pressure drops are almost always smaller, while the heat transfer coefficients are always larger under different sloshing conditions, which indicates that sloshing conditions can not only lead to drag reduction, but also bring about heat transfer enhancement. Moreover, the pitching condition shows the best drag reduction, followed by rolling condition, the worst in heaving condition; while the best heat transfer enhancement is found in heaving condition, followed by rolling condition, the worst in pitching condition.

Figures 6(a) and (b) display the variations of transient relative frictional pressure drop and heat transfer coefficient with time under different vapor qualities at heaving condition for C1C2C3, respectively. The results suggest that at heaving condition, the fluctuations of frictional pressure drop and heat transfer coefficient are both nearly sinusoidal, while the fluctuant magnitudes decrease with the increase of vapor quality. Meanwhile, compared to those at the static state, with the rise in vapor quality,

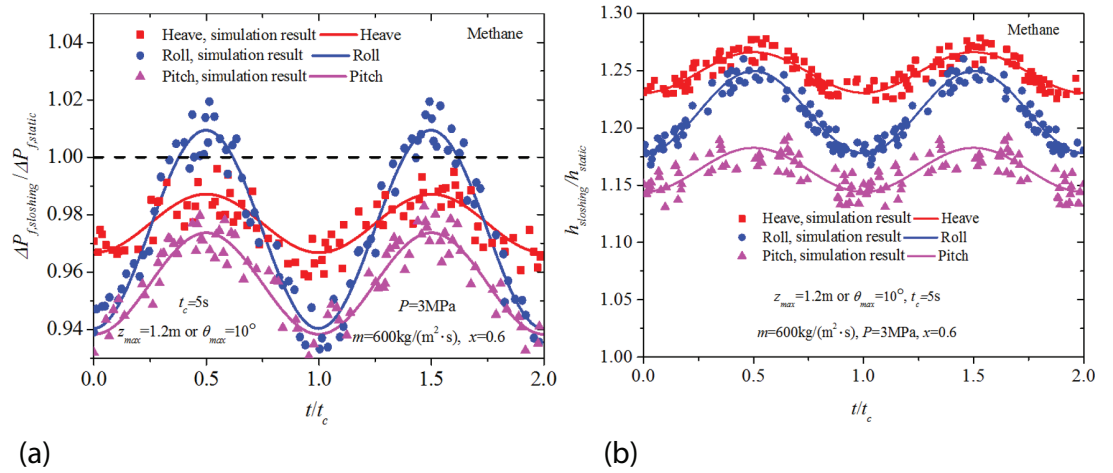


Figure 5: (a) Relative frictional pressure drop and (b) heat transfer coefficient versus time under different sloshing conditions for C1.

the time-averaged frictional pressure drop decrease about 6.45%, 9.26%, and 0.51%, respectively, while the time-averaged heat transfer coefficient increase about 12.77%, 4.46%, and 4.39%, respectively.

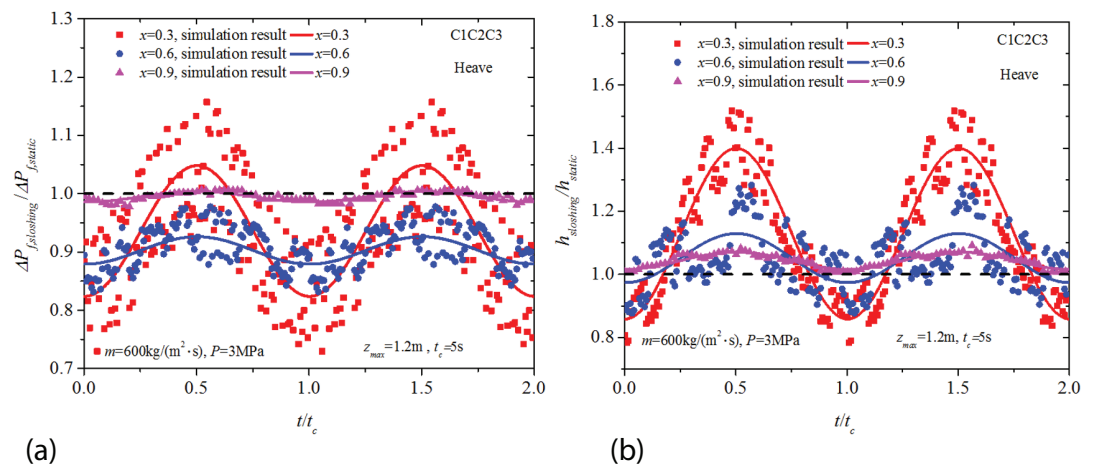


Figure 6: (a) Relative frictional pressure drop and (b) heat transfer coefficient versus time under different vapor qualities at heaving condition for C1C2C3.

4. Conclusion

The hydrocarbons condensation flow and heat transfer characteristics in a spiral pipe at static and sloshing conditions were numerically studied. Some key findings are drawn as:

1. Compared to methane/ethane/propane (C1C2C3), methane (C1) has better heat transfer, with smaller pressure drop.

2. At static conditions, as the vapor quality increases, the heat transfer coefficient first increases and then decreases, while the frictional pressure drop always increases.
3. Sloshing motion could cause both heat transfer enhancement and drag reduction.
4. With the rise in vapor quality, both pressure drop and heat transfer fluctuations become weakened.

Funding

The authors are grateful for the support of the research funds from 863 program on National high technology research and development program (2013AA09A216) and the program of the Ministry of Industry and Information Technology in China ([2013]418).

References

- [1] Li, S., Jiang, Y., Cai, W., et al. (2018). The influence of structural parameters on heat transfer and pressure drop for hydrocarbon mixture refrigerant during condensation in enhanced spiral pipes. *Applied Thermal Engineering*, vol. 140, pp. 759-774.
- [2] Li, S., Cai, W., Chen, J., et al. (2018). Evaluation analysis of correlations for predicting void fraction of condensation hydrocarbon refrigerant upward flow in a spiral pipe. *Applied Thermal Engineering*, vol. 140, pp. 716-732.
- [3] Wongwises, S. and Polsongkram, M. (2006). Condensation heat transfer and pressure drop of HFC-134a in a helically coiled concentric tube-in-tube heat exchanger. *International Journal of Heat and Mass Transfer*, vol. 49, no. 23-24, pp. 4386-4398.
- [4] Gupta, A., Kumar, R., and Gupta, A. (2014). Condensation of R-134a inside a helically coiled tube-in-shell heat exchanger. *Experimental Thermal and Fluid Science*, vol. 54, pp. 279-289.
- [5] Mozafari, M., Akhavan-Behabadi, M. A., Qobadi-Arfaee H, Fakoor-Pakdaman M: Condensation and pressure drop characteristics of R600a in a helical tube-in-tube heat exchanger at different inclination angles. *Applied Thermal Engineering*, 2015; 90: 571-578.
- [6] Salimpour, M. R., Shahmoradi, A., and Khoeini, D. (2017). Experimental study of condensation heat transfer of R-404A in helically coiled tubes. *International Journal of Refrigeration*, vol. 74, pp. 584-591.

- [7] Li, S., Cai, W., Chen, J., et al. (2018). Numerical study on the flow and heat transfer characteristics of forced convective condensation with propane in a spiral pipe. *International Journal of Heat and Mass Transfer*, vol. 117, pp. 1169–1187.
- [8] Li, S., Cai, W., Chen, J., et al. (2018). Numerical study on condensation heat transfer and pressure drop characteristics of ethane/propane mixture upward flow in a spiral pipe. *International Journal of Heat and Mass Transfer*, vol. 121, pp. 170–186.
- [9] Neeraas, B. O. (1993). Condensation of Hydrocarbon Mixtures in Coil-wound LNG Heat Exchangers, Tube-side Heat Transfer and Pressure Drop. PhD thesis, Norwegian Institute of Technology.
- [10] Tan, S., Su, G. H., Pu-Zhen, G. (2009). Heat transfer model of single-phase natural circulation flow under a rolling motion condition. *Nuclear Engineering and Design*, vol. 239, no. 10, pp. 2212–2216.
- [11] Yu, S., Wang, J., Yan, M., et al. (2017). Experimental and numerical study on single-phase flow characteristics of natural circulation system with heated narrow rectangular channel under rolling motion condition. *Annals of Nuclear Energy*, vol. 103, pp. 97–113.
- [12] Jin, G., Yan, C., Sun, L., et al. (2014). Effect of rolling motion on transient flow resistance of two-phase flow in a narrow rectangular duct. *Annals of Nuclear Energy*, vol. 64, pp. 135–143.
- [13] Chen, C., Gao, P., Tan, S., et al. (2015). Effect of rolling motion on two-phase frictional pressure drop of boiling flows in a rectangular narrow channel. *Annals of Nuclear Energy*, vol. 83, pp. 125–136.
- [14] Chen, C., Gao, P., Tan, S., et al. (2015). Effects of rolling motion on thermal-hydraulic characteristics of boiling flow in rectangular narrow channel. *Annals of Nuclear Energy*, vol. 76, pp. 504–513.
- [15] Lemmon, E. W., Huber, M. L., and McLinden, M. O. (2010). NIST Standard Reference Database 23: Reference Fluid Thermodynamic and Transport Properties-REFPROP. 9.0.